

Radio galaxies in the 2SLAQ Luminous Red Galaxy survey: II. The stellar populations of radio-loud and radio-quiet LRGs

Helen M. Johnston,^{1*} Elaine M. Sadler¹, Russell Cannon², Scott M. Croom¹,
Nicholas P. Ross^{3,4} and Donald P. Schneider⁴

¹*School of Physics, University of Sydney, NSW 2006, Australia*

²*Anglo-Australian Observatory, PO Box 296, Epping, NSW 1710, Australia*

³*Department of Physics, University of Durham, South Road, Durham DH1 3LE*

⁴*Department of Astronomy and Astrophysics, The Pennsylvania State University, 525 Davey Laboratory, University Park, PA 16802*

Accepted 2007 November 20. Received 2007 November 14; in original form 2007 September 19

ABSTRACT

We present an analysis of the optical spectra of a volume-limited sample of 375 radio galaxies at redshift $0.4 < z < 0.7$ from the 2dF-SDSS Luminous Red Galaxy and QSO (2SLAQ) redshift survey. We investigate the evolution of the stellar populations and emission-line properties of these galaxies. By constructing composite spectra and comparing with a matched sample of radio-quiet sources from the same survey, we also investigate the effect on the galaxy of the presence of an active nucleus.

The composite spectra, binned by redshift and radio luminosity, all require two components to describe them, which we interpret as an old and a younger population. We found no evolution with redshift of the age of the younger population in radio galaxies, nor were they different from the radio-quiet comparison sample. Similarly, there is no correlation with radio power, with the exception that the most powerful radio sources ($P_{1.4} > 10^{26}$ W/Hz) have younger stars and stronger emission lines than the less powerful sources. This suggests that we have located the threshold in radio power where strong emission lines “switch on”, at radio powers of around 10^{26} W/Hz. Except for the very powerful radio galaxies, the presence of a currently-active radio AGN does not appear to be correlated with any change in the observed stellar population of a luminous red galaxy at $z \sim 0.5$.

Key words: galaxies: active — galaxies: stellar content — cosmology: observations

1 INTRODUCTION

It is now accepted that most, if not all, massive galaxies host super-massive black holes at their centre. The observed tight correlation between the mass of the black hole and the global properties of the host galaxy (Magorrian et al. 1998; Gebhardt et al. 2000) suggests that the growth of the black holes at their centres is intimately related to the formation and assembly of these galaxies. However, at any one time only $\sim 5\%$ of galaxies are seen as powerful radio sources or show other evidence of an active galactic nucleus (AGN). The question arises: are the host galaxies of such AGN different from the hosts of inactive sources?

It has been known since the early 1960s that the hosts for powerful radio galaxies are massive ellipticals

(e.g. Matthews et al. 1964). The trigger for the transition from quiescence to an active state has been suggested to be gravitational interaction between galaxies. Signatures of tidal interactions are common amongst radio galaxies (e.g. Heckman et al. 1986), which presumably result in a large increase in the amount of material feeding the black hole, thus triggering the radio emission. Some individual radio galaxies also show significant association with young stellar populations (e.g. Aretxaga et al. 2001; Tadhunter et al. 2002; Wills et al. 2002; Johnston et al. 2005); this suggests that the merger process which triggers the radio emission can also lead to star formation in the host galaxy. However, numerical studies of galaxy interactions and mergers show that star formation is not necessarily enhanced, due to the amount of gas swept out (di Matteo et al. 2007).

Several questions remain to be answered in this scenario: What is the relationship among mergers, the trigger-

* E-mail: H.Johnston@physics.usyd.edu.au

ing of the active nucleus, and star formation: are all three components necessarily present? Do all early-type galaxies go through radio galaxy phases as they assemble?

In order to investigate these questions, we need to study a large and uniform sample of radio galaxies. Samples of this kind have recently been studied in the local universe ($z < 0.3$) by Best et al. (2005) and Mauch & Sadler (2007), but until now there has been no comparable sample available at higher redshift.

Best et al. (2005) investigated the properties of a sample of 2215 nearby radio galaxies (most with 1.4 GHz radio luminosity below 10^{25} W/Hz) from the Sloan Digital Sky Survey. They showed that the fraction of galaxies hosting a radio-loud AGN was a strong function of stellar mass, and that there was no correlation between radio luminosity and optical emission-line luminosity for the galaxies in their sample. Best et al. (2005) concluded that optical AGN and low-luminosity radio-loud AGN are independent phenomena which are triggered by different physical mechanisms. Mauch & Sadler (2007) studied a sample of 2661 radio-loud AGN selected from the 6dF Galaxy Survey. They confirmed the findings of Best et al. (2005) that radio-loud AGN preferentially inhabit the brightest and most massive host galaxies, and showed that the fraction of all galaxies which host a radio-loud AGN scales with the infrared K-band luminosity as L_K^2 .

We have constructed a volume-limited sample of radio sources by combining optical data from the 2SLAQ LRG survey (Cannon et al. 2006) with the radio data from the VLA FIRST survey (Becker et al. 1995). The 2SLAQ sample is focused on luminous red galaxies, thus pre-selecting for the large elliptical galaxies most likely to host powerful radio sources. Sadler et al. (2007) used this sample to study the evolution of the radio sources; in the current work, we investigate the properties of the host galaxies.

The signal-to-noise ratio of individual 2SLAQ spectra is adequate for redshift determinations, but is generally too low for accurate measurement of weak spectral features. We overcome this limitation by combining spectra to form composites. This approach allows us to investigate the variation of composites with both redshift and with radio power, and to address the key question: How does the stellar population of a galaxy correlate with the presence or absence of an active radio-loud AGN in its centre?

Throughout this paper, we use $H_0 = 71 \text{ km s}^{-1} \text{ Mpc}^{-1}$, $\Omega_m = 0.27$ and $\Omega_\Lambda = 0.73$.

2 DATA REDUCTION

2.1 Source selection

The source selection is discussed in detail in Sadler et al. (2007, Paper I); we present a brief summary here.

The 2SLAQ Luminous Red Galaxy survey (Cannon et al. 2006) consists of 14,978 spectra taken with the Two-degree Field instrument (2dF) on the 3.9m Anglo-Australian Telescope, of sources selected to have *ugriz* (Fukugita et al. 1996) photometry and non-stellar shape in the Sloan Digital Sky Survey (SDSS; York et al. 2000). The catalogue of sources with spectra was then cross-matched with the VLA FIRST catalogue (Becker, White & Helfand

1995) and the NVSS (Condon et al. 1998). These two surveys have complementary properties, with NVSS sampling the total flux density of extended sources, while FIRST has higher spatial resolution. Galaxies within 30 arcsec of a FIRST/NVSS source were flagged as possible matches (giving 2871 potential candidates). Optical images of the galaxies, primarily from Sloan Digital Sky Survey Data Release 3 (Abazajian et al. 2005), with a small number taken from the SuperCOSMOS Sky Surveys (Hambly et al. 2001), were compared visually with radio images from the FIRST survey. This process yielded 391 optical galaxies with 2SLAQ spectra which are true associations with radio sources. During this visual inspection, we also flagged and accounted for sources which are double and/or complex in structure.

Of these 391 radio sources, 14 had redshift quality values $Q < 3$, indicating a less-reliable redshift determination. These objects were excluded from further analysis; the remainder of the objects, with $Q \geq 3$, have redshift reliability $> 95\%$ (see Cannon et al. 2006, §5.4). The total radio detection rate was 2.7%. There were two sources in this list whose spectrum showed a measurable redshift but was significantly contaminated by a foreground star (the sources indicated as “M star plus galaxy” in Table 3 of Sadler et al. 2007). While these were usable for constructing a radio luminosity function, they would complicate our spectral modelling, so were removed from the sample for this paper, leaving 375 radio sources with optical spectra.

The total NVSS/FIRST radio flux of each object, including the flux from all separate components identified by eye, was converted to total radio power assuming $H_0 = 71 \text{ km s}^{-1} \text{ Mpc}^{-1}$ and $\Omega_M = 0.27$, using a k -correction of the form $(1+z)^{-(1+\alpha)}$ with $\alpha = -0.7$, which is the median radio spectral index (Mauch et al. 2003).

The final source list of 375 objects has redshifts ranging from $z = 0.31$ to 0.76, and radio power between $P_{1.4 \text{ GHz}} = 10^{23.44} \text{ W/Hz}$ and $10^{27.02} \text{ W/Hz}$. The redshift distribution of radio sources is shown in Fig. 1. The median redshift is $z = 0.54$, and the median radio power is $\log P = 24.60$.

2.2 Creation of a matched sample

To investigate the effect which the presence of an active nucleus has on its host galaxy, we must create a sample of non-radio galaxies, matched as closely as possible to the radio-loud sample. Since the probability that an early-type galaxy is a radio source is a strong function of optical luminosity (Auremma et al. 1977; Sadler et al. 1989), the radio galaxies in our sample are significantly more luminous than the 2SLAQ LRG sample as a whole, which makes careful matching imperative.

For each radio source, we selected a matching source from the remainder of the 2SLAQ catalogue. The sensitivity of the FIRST radio catalogue (with a typical flux density limit of 0.75 mJy; Becker et al. 1995) means that the upper limit to the radio power of these “radio-quiet” sources range between 10^{23} and 10^{24} W/Hz at 1.4 GHz. For each radio-loud object, we found the object best matched in redshift and r -magnitude by minimising the quantity

$$d = (z_{\text{RL}} - z_{\text{RQ}})^2 + (r_{\text{RL}} - r_{\text{RQ}})^2/20 \quad (1)$$

There are several possible ways of finding the “nearest”

radio-quiet galaxy; this expression was chosen empirically to weight the magnitude and redshift equally, so the resulting sample has roughly the same distribution in redshift and apparent magnitude. Since radio-loud sources make up only 2.7% of the LRG sample, this approach produces a sample which is well-matched to the radio-loud sources in redshift and apparent r magnitude. The maximum discrepancy between a radio source and its “matched” galaxy was 0.18 mag in apparent magnitude and 0.0067 in z , with 90% of sources having $\Delta r \lesssim 0.03$ mag and $\Delta z \lesssim 0.001$.

2.3 Spectral reduction

We began with the wavelength-calibrated spectra produced by the 2SLAQ project. These had a typical wavelength coverage of 5000–7250Å, which means that, at the redshift range of our targets, the region containing Ca II H and K and the 4000Å break is always covered. Although our spectra go well below 4000Å rest wavelength, our observational data are in the spectral region where instrumental and atmospheric effects on continuum slope are not severe. For redshifts beyond $z \sim 0.45$, H β and [O III] 5007 are shifted out of the 2dF wavelength range, so the most prominent emission line is [O II] 3727.

To combine the spectra, several steps of processing were applied to each spectrum. The regions around the strongest night sky features were removed and replaced by an interpolated value. We are hampered by the fact that the 2SLAQ spectra are not flux-calibrated, which means that the instrumental response can introduce changes in the slope of the continuum. We attempted to correct for this, at least in a mean sense, by dividing by an average response curve. We use the curve derived by Roseboom et al. (2007), which compared the 2SLAQ spectra of 160 galaxies which were also observed by the SDSS LRG survey (Eisenstein et al. 2001, 2003). We divided each spectrum by this response curve: since we are producing composite spectra this mean response curve should suffice, even though it does not take into account night-to-night variations. We then shifted each spectrum to the rest frame using the known redshift, and rebinned all the spectra onto the same scale, between 3280–4870Å, with a dispersion of 1.4Å/pixel

2.4 Creation of composites

The distribution of sources in $(z, \log P)$ is shown in Fig. 1. Although the redshifts range from $z = 0.31$ to 0.76, and the radio power from $\log P = 23.44$ to 27.02, the bulk of sources cluster near the middle of the range in each parameter. We thus had two choices: we can create composites with equal numbers of sources, which produces composites with equal signal-to-noise, or we can create composites within equal intervals in redshift or radio power, which maximises the baseline over which we can investigate changes, but at the expense of lowering the signal-to-noise ratio of the outlying composites.

We thus created *four* separate sets of composite spectra (Table 1, shown graphically by the dashed lines in Fig. 1):

(A) sort spectra by redshift and create 5 composites with equal numbers of sources: each composite is composed of 75 sources, and the redshift limits are shown in Table 1;

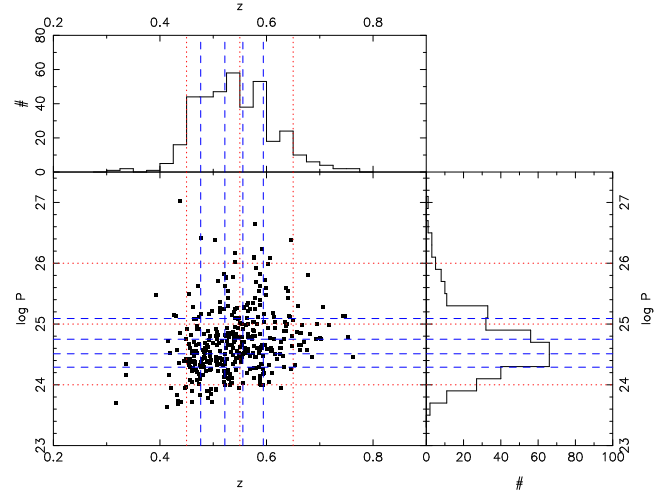


Figure 1. Distribution of sources in redshift and radio power at 1.4 GHz (measured in W/Hz). The separate histograms of redshift and radio power are shown above and to the right, respectively. The binning for the four separate sets of composites are indicated by the lines. Set A, binning by redshift with 75 sources in each bin, is shown by the vertical blue dashed lines; set B, binning by redshift with equal spacing, is shown by the vertical red dotted lines. Set C, binning by radio power with 75 sources in each bin, is shown by the horizontal blue dashed lines; set D, with equally spaced bins in radio power, is shown by the horizontal red dotted lines.

(B) sort by redshift and create 4 composites with equal spacing in redshift: this gave us four groups, with $z < 0.45$ (28 sources), $0.45 < z < 0.55$ (196 sources), $0.55 < z < 0.65$ (138 sources), and $z > 0.65$ (28 sources);

(C) sort by radio power and create 5 composites with equal numbers of sources: each composite is composed of 75 sources, and the redshift limits are shown in Table 1;

(D) sort by radio power and create 4 composites with equal spacing in radio power: this gives us four bins, with $\log P < 24$ (27 sources), $24 < \log P < 25$ (269 sources), $25 < \log P < 26$ (83 sources), and $\log P > 26$ (11 sources).

There are several different approaches which may be taken in combining low signal-to-noise ratio spectra to form composites: spectra may be weighted by the variance in each spectrum (e.g. Francis et al. 1991; Eisenstein et al. 2003), or weighted by luminosity (Baldry et al. 2002; Dressler et al. 2004); or the composite can be constructed from the median of individual spectra at each wavelength (Croom et al. 2002). Since the 2SLAQ galaxies are all intrinsically luminous red galaxies, we have taken the simplest approach and created composites by averaging the spectra in each group. The spectra were all taken with very similar wavelength coverage but have different redshifts, so in each rest wavelength bin, different numbers of spectra contribute to the sum, particularly for the highest and lowest redshifts. We corrected for this by counting the number of spectra which contribute at each wavelength and dividing the composite by this number.

The composite spectra were then normalised by the flux at 4050Å. Since the resolution of the spectral models we chose is 10Å (see § 3.2), we binned each composite into 20Å bins, and then removed bins which included the bright emis-

Table 1. Parameters of the composites and results of the fits. Four sets of composites A–D were created (see § 2.4 for details). Columns 1–4 show the name of the composite set, the range in redshift or radio power, and the number of spectra which went into each composite. The next three columns show the results of the spectra modelling (§ 3.2): the age of the young population, the fraction of light contributed by the young population at 4050Å, and the reduced χ^2_ν value for the best fit (for $\nu = 31$ degrees of freedom). Corresponding composites of a matched sample of radio-quiet sources (§ 2.2) were created, and the results of fitting to these are shown in columns 8–10.

Sample	#	Range	No. of galaxies	Radio-loud sample			Radio-quiet sample		
				Age (Myr)	Fraction	χ^2_ν	Age (Myr)	Fraction	χ^2_ν
(A) Redshift: equal numbers	1	$z = 0.31\text{--}0.48$	75	690	0.40	3.55	710	0.54	4.42
	2	$z = 0.48\text{--}0.52$	75	1000	0.47	3.61	1130	0.56	2.48
	3	$z = 0.52\text{--}0.56$	75	700	0.45	3.29	690	0.46	1.84
	4	$z = 0.56\text{--}0.59$	75	1120	0.55	1.32	670	0.50	0.87
	5	$z = 0.59\text{--}0.76$	75	1130	0.60	1.32	1120	0.70	1.55
(B) Redshift: equal spacing	1	$z = 0.31\text{--}0.45$	26	690	0.35	6.48	1110	0.57	2.00
	2	$z = 0.45\text{--}0.55$	192	700	0.40	3.26	1000	0.54	3.19
	3	$z = 0.55\text{--}0.65$	133	1120	0.66	1.26	1120	0.66	1.52
	4	$z = 0.65\text{--}0.76$	24	1130	0.64	0.94	1130	0.81	0.55
(C) Radio power: equal numbers	1	$\log P = 23.44\text{--}24.29$	75	720	0.50	3.61	710	0.53	2.68
	2	$\log P = 24.29\text{--}24.51$	75	1120	0.52	1.90	1010	0.59	1.42
	3	$\log P = 24.51\text{--}24.75$	75	710	0.45	1.94	710	0.64	6.45
	4	$\log P = 24.75\text{--}25.09$	75	700	0.47	2.06	1130	0.58	0.90
	5	$\log P = 25.09\text{--}27.02$	75	1140	0.53	1.06	700	0.56	1.90
(D) Radio power: equal spacing	1	$\log P = 23.44\text{--}24$	26	710	0.55	3.81	710	0.45	3.00
	2	$\log P = 24\text{--}25$	259	700	0.46	2.84	710	0.55	2.84
	3	$\log P = 25\text{--}26$	79	1130	0.51	0.81	990	0.64	1.77
	4	$\log P = 26\text{--}27.02$	11	110	0.46	1.61	680	0.59	0.68

sion lines, principally [O II] and [O III]. We estimated the errors on the flux in each wavelength bin by measuring the RMS of the 14 original pixels which were included in each 20Å bin. We chose to perform the fits to the models over the wavelength range 3500–4400Å, based on our desire to fit the same wavelength region in all spectra; a total of 33 independent data points in each spectrum were used in the fits.

Composites for the matched sample of radio-quiet sources (§ 2.2) were created in exactly the same manner; this data set serves as a control sample to see how the stellar population varies in the absence of a powerful radio source.

3 DATA ANALYSIS

3.1 Differences between composites

To determine if the presence of an active nucleus affects the galaxy, we compared the composites formed from the radio-loud sample and the matched radio-quiet sources (§ 2.2). The most basic test is to use a simple χ^2 test to find the probability that a pair of composites come from the same underlying distribution. Each of the eighteen radio-loud composite spectra (Table 1) was compared with the corresponding radio-quiet counterpart. All composites were consistent with being from the same distribution, except the D4 composite formed from the highest-power radio sources, where the $\chi^2_\nu = 3.5$. This initial evidence suggests that, with the exception of the very highest-power radio sources, there is no evidence of difference between galaxies containing an active AGN and those that do not.

3.2 Modelling the stellar continuum

We modelled the observed continuum as an old population plus a blue component due to a second population of stars of a younger age, using models from the GISSEL96 library (Bruzual A. & Charlot 1993). Of the models in their library, we used the ones with a Salpeter initial mass function with mass limits of 0.1 and 100 M_\odot and solar metallicity, using the Gunn & Stryker (1983) stellar spectral atlas.

We used two single-age stellar populations, representing instantaneous bursts of star formation. The old population was represented by a single-age population of age 7000 Myr, the younger stars by a population with a range of ages (10, 20, 50, 70, 100, 200, 500, 700, 1000, 2000 or 5000 Myr). The exact age of the “old” population is not critical, since the spectrum changes little at these ages; we chose 7 Gyr since at the highest redshift in our sample ($z = 0.76$) the age of the universe was 7 Gyr. We assembled the model spectra from the GISSEL96 library, and binned them to the same resolution as the observed spectra.

Since the observed continuum is modelled as the sum of two populations, we assumed each composite is represented as a 7000 Myr population plus some fraction f of a younger population with age τ ; our task is to determine f and τ for each composite. This parametrisation is unlikely to be a realistic representation of the stellar populations of these galaxies. However, the exact form of the models is not important, because our study is a *differential* test, comparing the properties of the radio-loud galaxies with their radio-quiet counterparts.

We created a 11 × 11 grid of model spectra. Along one axis, the age of the young population τ is varied between 10 Myr and 5 Gyr; along the other axis the fraction of light

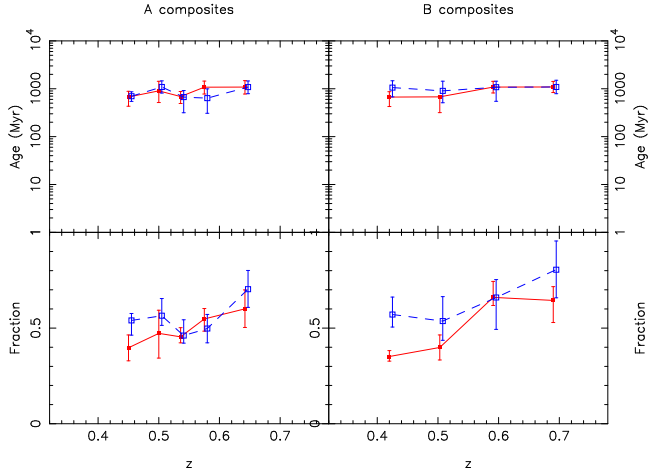


Figure 2. Results of fits to the A and B composites, showing the age and fraction of light contributed by young stars as a function of redshift. The red filled symbols (solid lines) represent the radio-loud sources, while the blue open symbols (dashed lines) represent the matched sample of radio-quiet sources; the radio-quiet sources have been offset slightly in redshift for clarity. The age of the young population does not change with redshift; the fraction of light contributed rises slightly.

contributed by the young population varies linearly between 0 and 100%. Thus the spectrum at grid position (5,3) consists of an old (7 Gyr) population plus a 100 Myr population, where the young population is contributing 20% of the light at 4050Å.

We calculated the χ^2 difference between the model spectrum and each of the observed composite spectra for all 121 model spectra. We allowed the normalisation of the model spectrum to vary between 0.75 and 1.25 of the flux of the observed spectrum at 4050Å, to allow for possible differences in slope between the model and the observed spectrum. This yields a χ^2 map for each observed composite; the best fit is chosen to be that where the χ^2 value is minimised.

The results of the fitting are shown in Table 1, and shown graphically in Figures 2 and 3. The best-fitting age and fraction were derived from a parabolic fit to the one-dimensional χ^2 curves through the minimum. The error bars represent the confidence interval given by the ellipse representing $\Delta\chi^2 = 3$ (containing $\sim 90\%$ of normally distributed data). In all cases, the χ^2 of the two-component model fit was significantly (\sim factor 2) better than the χ^2 of the fit using a single-aged stellar population.

The results of our modelling can be summarised as follows. There is no evolution with redshift of the stellar population of the radio galaxies, nor are they in any way different from radio-quiet galaxies matched in redshift and r luminosity. The age of the “young” population is unchanged with redshift, with our spectra requiring a second population of stars of age ~ 820 Myr over the whole redshift range of our sample. The fraction of light contributed by young stars is about 50%, and while it rises slightly over the redshift range of the sample, the change is not significant (1.4σ).

The B-composites and their best-fitting models are shown in Fig. 4.

We can also examine how the spectrum changes as a function of radio power, using the C and D composites de-

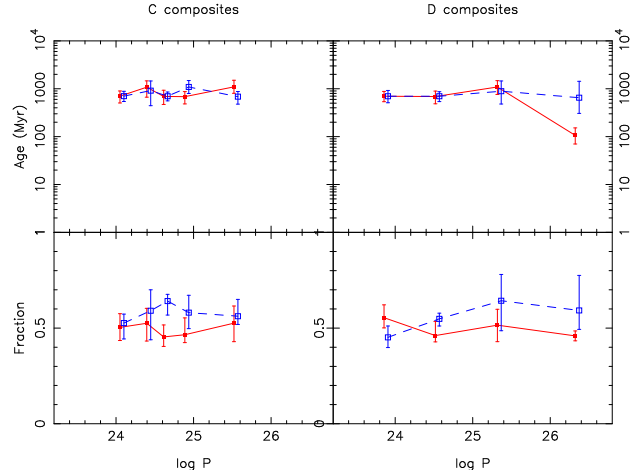


Figure 3. Same as Fig. 2, but for the C and D composites, showing the age and fraction of light contributed by young stars as a function of radio power. Neither the age of the young population nor the fraction of light contributed changes significantly as a function of radio power, *except* at the highest radio power (composite D4), where the second population is significantly younger.

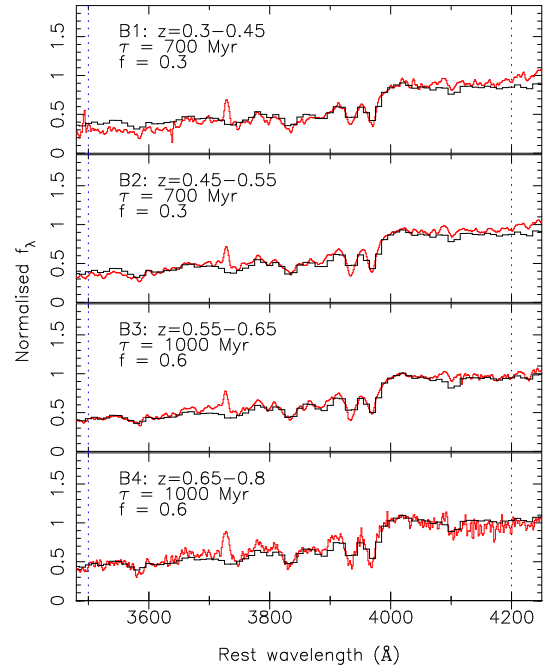


Figure 4. Model fits to the four B composite spectra, with equal spacing in redshift. The composite spectrum is shown in red, with the model fit, consisting of an old population plus a young population of age τ contributing a fraction f of the light at 4050Å, shown as the thick black line (Table 1). The dotted lines indicate the wavelength range over which the fitting was performed.

finer earlier. Again, our modelling shows no change in the age of the population or the fraction of young stars as the radio power increases (Fig. 3). The only exception is that the very highest power sources (the D4 composite, consisting of the 11 sources with $\log P > 26$; Table 1) appear to have a substantially younger population (100 Myr), as well as strong [O II] 3727 emission (which was not included in

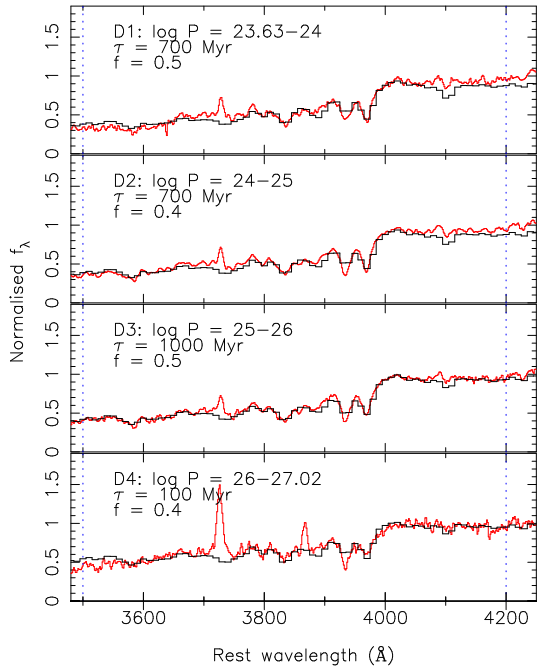


Figure 5. Model fits to the four D composite spectra, with equal spacing in radio power. The composite spectrum is shown in red, with the model fit shown as the thick black line (Table 1). Note the substantially stronger [O II] emission line in the highest radio power spectrum (composite D4), as well as [Ne III] emission.

the fit). This difference is not seen in the matching sample of radio-quiet sources, suggesting that the young stars are in some way associated with the active nucleus. Recall that this was the only composite showing a simple χ^2 difference with the other composites (§ 3.1). We checked the eleven individual spectra which went into the D4 composite, in case the composite was being skewed by a single peculiar object. No individual spectrum appeared to be peculiar; 6 of the 11 showed strong emission lines. The D-composites and their best-fitting models are shown in Fig. 5. We tried splitting the second-highest power bin (D3), to see if there was a continuous trend; both sub-bins had similar ages, of ~ 1000 and ~ 700 Myr, quite different from the 100 Myr population found in the D4 bin. Thus the difference appears to be confined to the very highest radio-power sources.

In Figure 6 we plot the ratio of these models. The figure shows there are small changes to spectral lines, but the principal difference is a change in slope in the model fit to the D4 composite.

We investigated whether the young population in the highest-power radio sources could in fact be due to emission from the central AGN, which would also produce excess blue light. We tried replacing the second, young population in our fits with a power-law continuum of the form $f_\lambda \propto \lambda^\alpha$, where α was allowed to vary between -5 and 0 . The fit was significantly poorer than the best-fitting model with a young stellar population: the 4000\AA break was not well reproduced. Thus we conclude that the highest power radio sources do show evidence of association with a population of young stars.

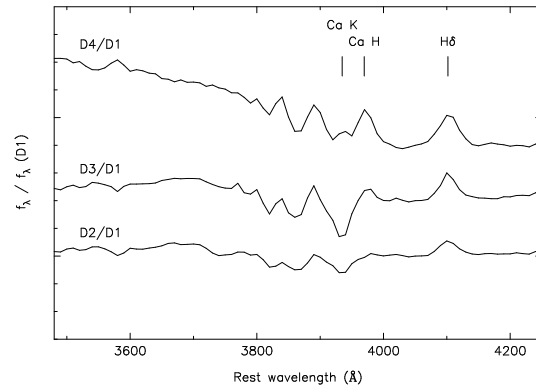


Figure 6. Comparison between the model fits to the four D composite spectra (Fig. 6). The models are shown divided by the best-fit model to the D1 composite ($\tau = 500$ Myr, $f = 0.5$), and offset in the vertical direction for clarity.

3.3 Emission lines

Emission lines were present in many of the spectra, mostly [O II], and occasionally [Ne III] and [Ne V] (see Table 3 of Sadler et al. 2007). The [O III] 4958,5007 pair was seen in only a single galaxy, J100322.41-000137.8, but was redshifted beyond the wavelength range of most of our sources. Sadler et al. (2007) found that the fraction of 2SLAQ radio galaxies which show [O II] emission is higher (27%) than the overall 2SLAQ spectroscopic sample (17.7%; Roseboom et al. 2006). However, since more luminous galaxies are more likely to show emission, this result needs to be approached with caution. In any case, most of the radio galaxies in 2SLAQ would not have been recognised as AGN on the basis of their optical spectra alone. This agrees well with several other studies, which found little evidence of correlation between radio power and emission line strength in nearby radio galaxies (Rixon et al. 1991; Owen et al. 1995).

By using a comparison sample of radio-quiet galaxies, matched in redshift and luminosity, we are able to investigate this effect. Comparison of the emission-line properties of our radio-loud sources with the matched sample of radio-quiet galaxies reveals differences between the two groups. We can examine the emission lines in two ways: finding the number of individual galaxies which show emission lines as a function of various parameters, and investigating the properties of the emission lines in the composite spectra.

3.3.1 Emission lines in individual sources

The equivalent widths of the [O II] line in the individual spectra were measured using the SPECFIT package implemented in IRAF (Kriss 1994). We normalised the spectra by a spline fit to the continuum, then measured the equivalent width of the emission line by fitting a Gaussian profile to the line. We must be careful to account for sources where the emission line fell on a sky line, or was redshifted out of the spectrum, and so would not have been detected if it were present. There were 333 sources in which [O II] was potentially detectable, with sources at redshifts ~ 0.48 and ~ 0.58 most strongly affected when the [O II] line fell on a bright sky line.

Following Sadler et al. (2007), we used a rest equivalent width cutoff of 7\AA to define sources with [O II] emis-

sion. Using this criterion, 50 out of the 333 (15%) radio-loud sources in which [O II] emission was potentially detectable show such emission, compared to 25 out of the matched radio-quiet sample (7.5%); so the radio-loud sources are significantly more likely to show [O II] emission than galaxies matched in optical luminosity and redshift. If we assume the fraction of radio-quiet galaxies showing emission represents the null-hypothesis (25/333), then observing 50/333 radio-loud sources with emission is highly significant ($p \ll 0.001$). For the [Ne III] 3869 and [Ne V] 3426 lines, we used a cut-off of $W_\lambda > 4\text{\AA}$ to define the emission-line sources. There were 25 sources with [Ne III] emission and 15 with [Ne V] emission in the radio-loud sample, compared to 11 and 8 respectively in the radio-quiet sample. Again, the radio-loud sources are roughly twice as likely to show emission than their radio-quiet counterparts (probability $p < 0.001$ and 0.05 respectively). Twenty-one radio-loud sources have $W_\lambda([\text{O III}]) > 15\text{\AA}$, compared with just five sources among the radio-quiet galaxies.

There is a slight trend for the fraction of sources showing emission to increase with redshift. In Fig. 7 we plot the fraction of sources which show [O II] emission (out of those in which it was potentially detectable) as a function of redshift. A similar trend is seen in the radio-quiet sources. This could be an absolute magnitude effect, as we are selecting slightly more luminous galaxies at higher redshift (Sadler et al. 2007).

[O II] emission is seen in radio galaxies at all radio powers (though it is somewhat more common in low- ($\log P < 24.5$) and high-power ($\log P > 25$) sources, as shown in the right-hand panel of Fig. 7). ‘‘Strong’’ [O II] emission, however, with $W_\lambda > 15\text{\AA}$, is significantly more common in the highest-power radio galaxies: 28% of sources with $\log P > 25.5$ (9 out of 35) have $W_\lambda > 15\text{\AA}$ compared to $\sim 3\%$ of sources at lower radio power. [Ne III] and [Ne V] emission is also more common at higher radio power. Neither of these trends can be seen in the sample of radio-quiet sources which match the distribution of the radio galaxies in z and r .

3.3.2 Emission lines in the composite spectra

By combining many spectra, we can measure changes in line ratios much more accurately than we can in individual sources.

We measured the line properties of the emission lines in the composite spectra by fitting Gaussian profiles using SPECFIT again, using the same technique as in §3.3.1. The spectra were normalised by a spline fit to the continuum, and then Gaussians were fit, constraining the wavelengths to be within $\pm 5\text{\AA}$ of the known wavelengths of the lines. These fits are shown in Figure 8; the line properties are listed in Table 2.

There is little difference in the emission lines of the composite spectra until the very highest radio-power is reached. This composite shows much stronger [O II] emission, as well as strong [Ne V] and [Ne III] emission lines, lines which are characteristic of quasars. The radio-quiet galaxies which are matched in luminosity and redshift show no increase in [O II] emission, and no trace of neon lines. This is not just due to the contribution from a single source: three of the nine sources with highest radio power have $W_{3426} > 4\text{\AA}$ (in

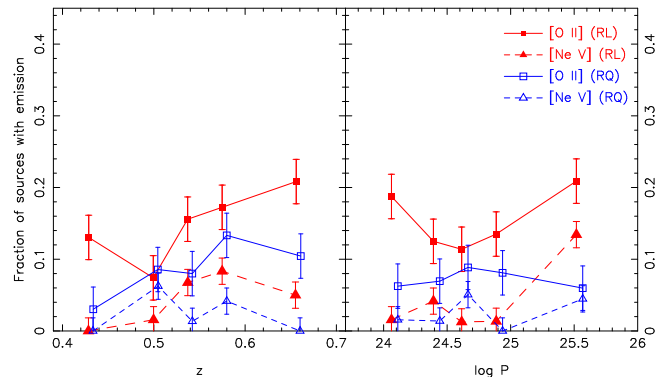


Figure 7. Fraction of sources with [O II] and [Ne V] emission, as a function of redshift and radio power; $\log P$ is defined for the radio-quiet sample by the matching to the radio-loud sources (§ 2.2). The red filled symbols represent the radio-loud sources (RL), while the blue open symbols represent the matched sample of radio-quiet sources (RQ). The squares and solid lines show the fraction of sources with $\text{EW}([\text{O II}] 3727) > 7\text{\AA}$, the triangles and dashed lines show the fraction of sources with $\text{EW}([\text{Ne V}] 3426) > 4\text{\AA}$. The radio-loud sources show a higher fraction of sources with emission than the radio-quiet sources, as well as a tendency for this fraction to increase with redshift. The likelihood of showing emission increases with radio-power (right-hand panel), especially for the [Ne V] emission.

Table 2. Equivalent widths of the fits to the emission lines in the D composites (Fig. 8) The equivalent widths of the three emission lines are shown, for the radio-loud and matched radio-quiet composites. The last two lines show the fits to the Neon composite and the [O II] composite (§3.3.2).

Composite	[O II] 3727 (\AA)	[Ne V] 3426 (\AA)	[Ne III] 3869 (\AA)
Radio loud D1	4.2 ± 0.7	< 1.0	0.9 ± 0.7
Radio loud D2	3.7 ± 0.4	1.0 ± 0.4	1.0 ± 0.4
Radio loud D3	3.3 ± 0.4	< 0.5	1.4 ± 0.4
Radio loud D4	14.1 ± 0.6	6.8 ± 0.5	5.2 ± 0.4
Radio quiet D1	1.5 ± 0.4	< 0.5	< 0.6
Radio quiet D2	2.1 ± 0.3	< 0.4	1.2 ± 0.4
Radio quiet D3	2.2 ± 0.3	< 0.3	1.5 ± 0.4
Radio quiet D4	1.8 ± 0.5	1.9 ± 0.9	1.0 ± 0.9
Neon composite	17.2 ± 0.7	7.9 ± 0.6	8.1 ± 0.6
[O II] composite	17.7 ± 0.9	< 0.7	1.8 ± 0.6

two sources the line fell on a sky line). This result implies that the increased emission seen in the most powerful radio sources is not just a function of galaxy size, but is tied to the activity of the central black hole.

Owen et al. (1995) and Best et al. (2005), found no correlation between radio power and emission line properties; their samples only reached radio powers $P \sim 10^{25}$ W/Hz. The emission-line luminosity of very powerful radio sources is known to correlate with radio power (e.g. McCarthy 1993, Fig. 2). There must be a threshold radio power at which strong emission lines ‘‘switch on’’ at a level above the usual incidence in quiescent galaxies; at the highest radio luminosities, virtually every radio galaxy has strong forbidden lines (Hine & Longair 1979). Our results suggest we have found this threshold, at radio powers of around 10^{26} W/Hz.

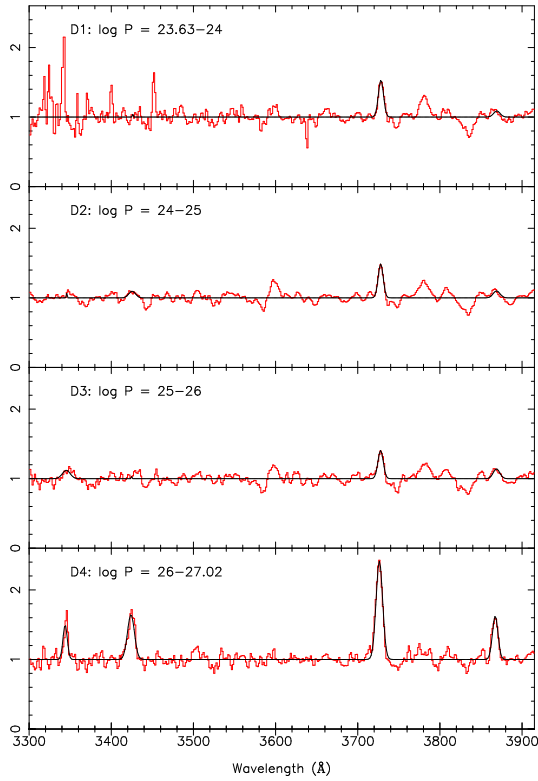


Figure 8. Gaussian fits to the emission lines in the D composites, with equal spacing in radio power. The normalised composite spectra are shown in red, and the Gaussian fits to the emission lines are shown as the thick black line. [O II] emission is seen at all radio powers, though it is significantly stronger in the highest power sources; these are the only ones to show significant [Ne V] and [Ne III] emission. The fourth line is a weaker [Ne V] line at 3346Å. The blue end of the lowest-power composite is noisy, because the lowest-power sources are only found at nearby redshifts, so there is not much signal at short wavelengths in this composite.

As noted earlier (§ 3.3.1), there were 21 sources which showed strong [O II] emission, with $W_\lambda > 15\text{\AA}$. There were also 32 sources which showed [Ne III] and/or [Ne V] emission. There was not total overlap between these: there were ten sources which showed strong [O II] emission but no [Ne III]/[Ne V] emission. To test whether this difference was real, we constructed two composite spectra: (a) the 32 sources which showed [Ne V] and/or [Ne III] emission (the “Neon composite”), and (b) the sources that showed strong [O II] emission but no [Ne III] or [Ne V] emission (the “[O II] composite”). We could only use five of the ten sources without [Ne III]/[Ne V] emission in constructing the [O II] composite, because the other five had at least one of the three neon lines falling on a sky line. The composites are shown in Figure 10.

Clearly these two composites have significantly different line ratios: the non-detection of [Ne V] in some sources is not just a signal-to-noise ratio issue. The Neon composite has line ratios $[\text{Ne V}]/[\text{O II}] = 0.46 \pm 0.03$ and $[\text{Ne III}]/[\text{O II}] = 0.47 \pm 0.03$, while the [O II] composite has $[\text{Ne V}]/[\text{O II}] < 0.04$ and $[\text{Ne III}]/[\text{O II}] = 0.10 \pm 0.03$. This suggests different ionisation mechanisms are operating in these two groups. For comparison, the composite quasar spectrum published by

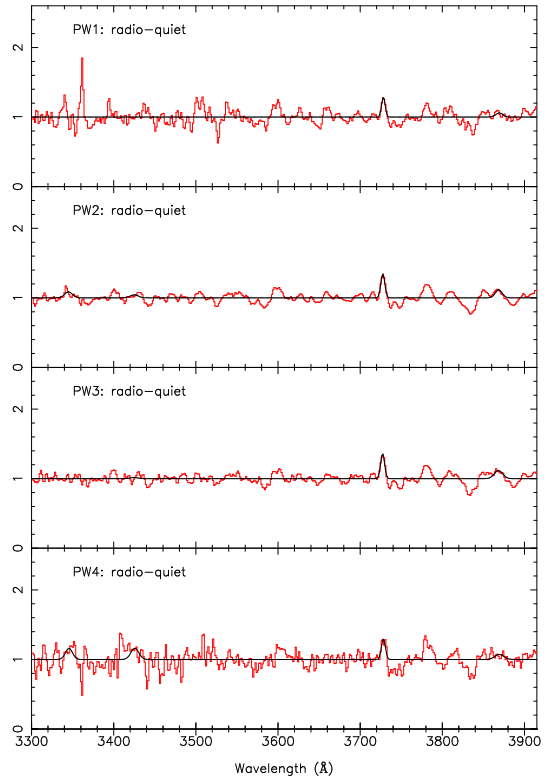


Figure 9. Same as Fig. 8, but for the matched radio-quiet composites. Clearly the emission line properties are very different to the radio-loud sources, with no detectable [Ne V] or [Ne III] emission.

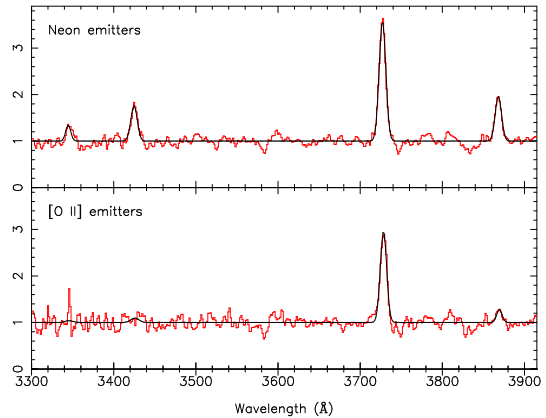


Figure 10. Gaussian fits to the emission lines in composites of sources which show significant [Ne V] and [Ne III] emission, and sources which show strong [O II] emission but no [Ne V] or [Ne III] emission. Only sources where all emission lines were clear of the night sky lines were included.

Vanden Berk et al. (2001) has ratios $[\text{Ne V}]/[\text{O II}] = 0.78 \pm 0.02$ and $[\text{Ne III}]/[\text{O II}] = 0.88 \pm 0.02$.

We investigated whether the stellar continuum in these emission line composites were at all different; nothing definitive could be found. The [O II] composite required a higher proportion of young stars to model the continuum than the Neon composite (80% compared to 40%), but this was only

marginally significant; there were only five spectra in the [O II] composite.

4 CONCLUSIONS

We have investigated the optical properties of a volume-limited sample of radio galaxies in the 2SLAQ Luminous Red Galaxy survey. We created composite spectra in order to investigate how the stellar populations of these galaxies depend on redshift or radio power. By constructing a comparison sample of galaxies matched in redshift and luminosity, we can eliminate the possibility that any effects we find are a result of the fact that radio-loud galaxies are on the average more luminous than radio-quiet galaxies.

We modelled the underlying starlight using single-age stellar population models. None of the spectra were adequately described by a single model; they all demanded an additional stellar component. We achieved satisfactory fits assuming that each spectrum consisted of an “old” (7 Gyr) population plus a fraction of light contributed by a “young” population, whose age was allowed to vary between 10 Myr and 5 Gyr. Neither a power-law component nor a model with continuous star formation described the spectra as well as the two-stellar population model.

The stellar populations of all the composites were almost identical, independent of redshift, radio power, and whether or not the galaxy contains an active radio source. The fraction of light contributed by the young population ($\sim 40\%$ at 4050\AA) increased marginally with redshift, but is not correlated with radio power. The age of the “young” component was consistent with an age of 1000^{+1000}_{-500} Myr for all composites. The sole exception was the composite made from the eleven most powerful radio sources, with $\log P > 26$, which was fitted with a young population of age 100 Myr. This was not seen in the corresponding composite of radio-quiet sources, which means it is unlikely to be due to a systematic effect, which would affect both radio-loud and radio-quiet galaxies equally. In addition, Sadler et al. (2007) showed that the median redshift of 2SLAQ radio galaxies is independent of radio power, so there are unlikely to be subtle aperture effects affecting the sample.

The two-population model is probably not a very realistic description of the underlying stellar light. However, our study is a *differential* test, comparing the properties of the radio-loud galaxies with their radio-quiet counterparts. In a future paper, we will investigate other models to represent the stellar populations of these galaxies.

The emission line properties of the population show more correlation with radio activity. Approximately 15% of the radio-loud sources show significant [O II] emission, compared to 7.5% of the radio-quiet sample; similarly, the radio-loud sources were roughly twice as likely to show [Ne III] and/or [Ne V] emission than their radio-quiet counterparts (12% and 6%, respectively). Still, it is notable that most of the radio galaxies in the 2SLAQ would not have been recognised as AGN on the basis of their optical spectra alone. The different [O II]/Ne line ratios seen in different objects suggest there is more than one emission mechanism operating to ionise the gas: these are likely to include hot stars and post-AGB stars as well as ionisation by the central AGN.

These observations support the model that all luminous

red galaxies contain a central black hole, only some of which are active at any one time; the current activity of the central black hole, as measured by the radio emission, does not appear to correlate with the stellar population in the galaxy. The sole exception appears to be that the most powerful radio galaxies show more activity and younger stars than the rest of the population. Even so, with young (~ 100 Myr) stars contributing 30% of the light, the fraction of mass in young stars is only 0.5% of the mass of the galaxy.

We need to be careful to distinguish between differences related to the activity of the central black hole and luminosity effects, since more massive galaxies are more likely to harbour AGN. We controlled for this bias by constructing a matched sample of radio-quiet galaxies. The comparison sample is matched in redshift and apparent magnitude, so the radio-quiet galaxies match the radio-loud sources closely in absolute luminosity. Since we saw differences in the most powerful radio galaxies, but not in their radio-quiet counterparts, the difference most likely relates to the presence of an active black hole. In Paper I, the 2SLAQ radio galaxies were found to cluster more strongly than the 2SLAQ LRG population as a whole (Sadler et al. 2007). It was speculated in that paper that this might be a luminosity effect, since the 2SLAQ radio galaxies are more luminous than the rest of the sample. However, recent work using samples matched in luminosity suggest this is not the explanation (Wake et al., in prep.). This suggests the radio galaxies really are preferentially located in denser environments, with more gas available to feed the black hole. Best et al. (2007) have recently suggested that a similar effect is seen in lower-redshift radio galaxies from SDSS.

Our results support the findings of Best et al. (2005), who found that the probability that a galaxy is radio-loud is independent of whether it is optically classified as an AGN, and that the host galaxies of radio-loud AGN match their radio-quiet counterparts. If optical emission lines trace current feeding of black holes, while radio emission points to mostly dormant black holes, accreting at low rates, then the current rate of growth of black holes in these galaxies is very low.

One notable point is that the age of the “young” population remains unchanged at 700 Myr (Table 1) despite the different ages of the galaxies: the highest redshift galaxies in our sample ($z = 0.76$) are 3.1 Gyr younger than the lowest redshift galaxies ($z = 0.31$). If the stellar populations in the lowest redshift galaxies were born 1 Gyr before $z = 0.31$, we should see the era of star birth, since it is covered in our sample (at a redshift $z = 0.39$). We see no evidence, however, for an epoch of star formation at that redshift.

So where are the galaxies which are forming stars as we observe them? There are two possibilities. If the single-age stellar population is a bad assumption, we may have low-level ongoing star-formation instead of star formation in discrete bursts. The second possibility, however, is that the initial colour selection of the 2SLAQ sample is biased towards accepting galaxies with these ages; in other words, the counterparts of our $z = 0.3$ galaxies are indeed forming stars at $z = 0.4$, but they don’t appear as red galaxies while forming stars, so are not included in the 2SLAQ sample.

In fact, our modelling suggests that we may not notice these galaxies using the 2SLAQ *gri* colour selection criteria. A model galaxy with 5% of the mass in young stars formed in

a single burst (which contributes 40–50% of the light around 1 Gyr after the burst) is only 1 mag bluer than the bulk of old galaxies. Furthermore, since most of the colour evolution occurs very early on, in the first 50 Myr, the chances of finding such an object in our sample is not high. In order to locate these galaxies, we would need to assemble a large sample of luminous galaxies using a different colour selection.

ACKNOWLEDGMENTS

We would like to thank the referee, Jasper Wall, for his extremely helpful comments and suggestions. Funding for the SDSS and SDSS-II has been provided by the Alfred P. Sloan Foundation, the Participating Institutions, the National Science Foundation, the U.S. Department of Energy, the National Aeronautics and Space Administration, the Japanese Monbukagakusho, the Max Planck Society, and the Higher Education Funding Council for England. The SDSS Web site is <http://www.sdss.org/>. This work was partially supported by National Science Foundation grant AST-0607634 (N.P.R.).

REFERENCES

- Abazajian K., et al. 2005, *AJ*, 129, 1755
 Aretxaga I., Terlevich E., Terlevich R. J., Cotter G., Díaz Á. I., 2001, *MNRAS*, 325, 636
 Auremma C., Perola G. C., Ekers R. D., Fanti R., Lari C., Jaffe W. J., Ulrich M. H., 1977, *A&A*, 57, 41
 Baldry I. K., et al. 2002, *ApJ*, 569, 582
 Becker R. H., White R. L., Helfand D. J., 1995, *ApJ*, 450, 559
 Best P. N., Kauffmann G., Heckman T. M., Brinchmann J., Charlot S., Ivezić Ž., White S. D. M., 2005, *MNRAS*, 362, 25
 Best P. N., von der Linden A., Kauffmann G., Heckman T. M., Kaiser C. R., 2007, *MNRAS*, 379, 894
 Bruzual A. G., Charlot S., 1993, *ApJ*, 405, 538
 Cannon R., et al. 2006, *MNRAS*, 372, 425
 Condon J. J., Cotton W. D., Greisen E. W., Yin Q. F., Perley R. A., Taylor G. B., Broderick J. J., 1998, *AJ*, 115, 1693
 Croom S. M., et al. 2002, *MNRAS*, 337, 275
 di Matteo P., Combes F., Melchior A.-L., Semelin B., 2007, *A&A*, 468, 61
 Dressler A., Oemler A., Poggianti B. M., Smail I., Trager S., Shectman S. A., Couch W., Ellis R., 2004, *ApJ*, 617, 867
 Eisenstein D. J., et al. 2001, *AJ*, 122, 2267
 Eisenstein D. J., et al. 2003, *ApJ*, 585, 694
 Francis P. J., Hewett P. C., Foltz C. B., Chaffee F. H., Weymann R. J., Morris S. L., 1991, *ApJ*, 373, 465
 Fukugita M., Ichikawa T., Gunn J. E., Doi M., Shimasaku K., Schneider D. P., 1996, *AJ*, 111, 1748
 Gebhardt K., et al. 2000, *ApJ*, 543, L5 p
 Gunn J. E., Stryker L. L., 1983, *ApJS*, 52, 121
 Hambly N. C., et al. 2001, *MNRAS*, 326, 1279
 Heckman T. M., Smith E. P., Baum S. A., van Breugel W. J. M., Miley G. K., Illingworth G. D., Bothun G. D., Balick B., 1986, *ApJ*, 311, 526
 Hine R. G., Longair M. S., 1979, *MNRAS*, 188, 111
 Johnston H. M., Hunstead R. W., Cotter G., Sadler E. M., 2005, *MNRAS*, 356, 515
 Kriss G. A., 1994, in Crabtree D. R., Hanisch R. J., Barnes J., eds, *Astronomical Data Analysis Software and Systems III* Vol. 61 of ASP Conference Series, Fitting models to UV and optical spectra using SPECFIT in IRAF. ASP, San Francisco, pp 437–446
 McCarthy P. J., 1993, *ARA&A*, 31, 639
 Magorrian J., et al. 1998, *AJ*, 115, 2285
 Matthews T. A., Morgan W. W., Schmidt M., 1964, *ApJ*, 140, 35
 Mauch T., Murphy T., Buttery H. J., Curran J., Hunstead R. W., Piestrzynski B., Robertson J. G., Sadler E. M., 2003, *MNRAS*, 342, 1117
 Mauch T., Sadler E. M., 2007, *MNRAS*, 375, 931
 Owen F. N., Ledlow M. J., Keel W. C., 1995, *AJ*, 109, 14
 Rixon G. T., Wall J. V., Benn C. R., 1991, *MNRAS*, 251, 243
 Roseboom I. G., et al. 2006, *MNRAS*, 373, 349
 Roseboom I. G. et al. 2007, *The 2dF-SDSS LRG and QSO survey: the cosmic evolution of Luminous Red Galaxies*, *MNRAS*, in prep.
 Sadler E. M., et al. 2007, *MNRAS*, 381, 211
 Sadler E. M., Jenkins C. R., Kotanyi C. G., 1989, *MNRAS*, 240, 591
 Tadhunter C., Dickson R., Morganti R., Robinson T. G., Wills K., Villar-Martin M., Hughes M., 2002, *MNRAS*, 330, 977
 Vanden Berk D. E., et al. 2001, *ApJ*, 122, 549
 Wills K. A., Tadhunter C. N., Robinson T. G., Morganti R., 2002, *MNRAS*, 333, 211
 York D. G., et al. 2000, *AJ*, 120, 1579